

# High-Energy 6.2-fs Pulses for Attosecond Pulse Generation

S. Ghimire, B. Shan, C. Wang, and Z. Chang

Department of Physics, Macdonald Laboratory, Kansas State University, Manhattan, KS 66506, USA

e-mail: chang@phys.ksu.edu; sghimire@phys.ksu.edu

Received January 1, 2005

**Abstract**—We explored a novel approach for increasing the energy of few-cycle laser pulses generated by using the hollow-core fiber/chirped mirror compressor technique. Our experiments showed that, when input pulses are circularly polarized, the output energy could be scaled up by a factor of 1.5 in comparison to that with a linear polarization input. Furthermore, the spectral width of output pulses is broader when the input pulses are circularly polarized, which yields 6.2-fs pulses. The results are explained by the suppression of ionization with a circular polarization input.

Attosecond XUV pulses are important tools for studying electron dynamics in atoms and molecules [1–4]. High-order harmonic generation is an effective process for the generation of single attosecond pulses [4, 5] or a train of attosecond electromagnetic bursts [2, 6]. We have proposed and reported the generation, by using the polarization gating technique, of an XUV supercontinuum that supports a single attosecond pulse in a broader plateau region [7, 8]. In the experiment, a pulse with a time-dependent ellipticity was formed by combining a left-circularly polarized pulse and a delayed right-circularly polarized pulse. In such a pulse, the polarization varies from circular to linear and then back to circular. Using the ellipticity-dependent pulse, the oscillating electron on an atom will be driven away from the parent ion at both the leading and trailing regions by the transverse component of the field. Therefore, high-order harmonics could only be produced in the center region of the composite pulse, which was called the polarization gate. The gate width was calculated as [7]

$$\delta t \approx 0.3 \frac{\tau_p^2}{T_d}, \quad (1)$$

where  $\tau_p$  is the pulse duration of the circular pulses and  $T_d$  is the delay between them. The duration of the circularly polarized laser pulses should be as short as possible to reduce the width of the polarization gate. It is clear that reducing the pulse duration is more effective than increasing the time delay to achieve the required polarization gate width. Using few-cycle laser pulses also avoids significant ionization of the atom by the leading edge of the pulse. The polarization gating is more effective for high harmonic orders because they are more sensitive to the ellipticity of the laser. The generation of higher order harmonics requires energetic laser pulses.

The hollow-core fiber/chirped mirror compressor is one of the most effective ways to generate few-cycle laser pulses [9, 10] with output energy up to ~0.5 mJ

[10]. Both theoretical [11, 12] and experimental studies [9] have been done to understand the constraints for obtaining more energy out of this technique. It is believed that multiphoton ionization [1] and self-focusing are the two dominating factors that limit the maximum input energy before the spatial mode of the output beam breaks. On one hand, the ionized gas can cause the laser beam to defocus in the region close to the entry of the fiber and inside the fiber. On the other hand, the self-focusing can transfer the energy of the pulse from the fundamental fiber mode to the higher order modes [12]. The interplay between plasma defocusing and self-focusing makes the process even more complicated. Some efforts have been devoted to scaling up the output energy. For example, a method of using a differential pumping technique was proposed in [11]. Here, we study another method for increasing the output energy.

Both multiphoton ionization and self-focusing (the optical Kerr effect) are nonlinear processes. For the same laser energy, the electric field strength is less for circular light than for linear light. The nonlinear processes are weaker when the input pulses are circularly polarized due to reduction in the field strength. Because of the reduction in the field strength, both nonlinear processes are weaker when the input pulses are circularly polarized. Thus, we expected that the fiber could work at a higher input energy level. The experiment was done with input energies up to 1.3 mJ from the *Kansas Light Source* [13], which operates at a repetition rate of 1 kHz at a central wavelength of 780 nm. We characterized the input pulses by using a single-shot, second-harmonic generation frequency-resolved optical gating (SHG-FROG) [14]. The FROG setup is shown in Fig. 1. Ten percent of the beam was diverted to the SHG-FROG, where it was split evenly into two parts with a broadband 50/50 beam splitter. The reflected beam, after passing through a compensating plate, and the transmitted beam were overlapped spatially as well as temporally onto a 5- $\mu$ m-thick, type-I BBO crystal (phase-matching angle of  $\theta = 29.2^\circ$ ) for the second-harmonic

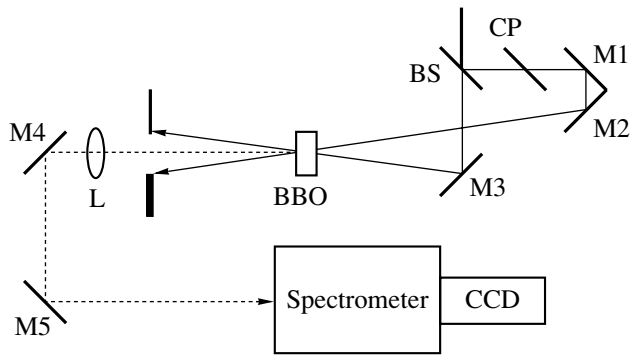


**Fig. 1.** Schematic of the SHG-FROG. The solid line represents a fundamental beam, and the dotted line represents the second-harmonic beam. BBO is a type-I phase-matching crystal with 5- $\mu\text{m}$  thickness. BS is a beam splitter, and CP is a compensating plate. M1, M2, and M3 are silver mirrors. M4 and M5 are UV-enhanced aluminum mirrors.

generation. The second-harmonic signal was then spatially filtered out from the fundamental beam and diverted to a spectrometer with a UV CCD camera as a detector. The crystal was imaged onto the entrance slit of the spectrometer with a lens of focal length 250 mm and a demagnification of 1/2. Finally, a commercially available FROG algorithm (Femtsoft Technologies Ver. 3.1.2) was used to reconstruct the original pulse from the measured FROG trace. The FWHM of the measured pulse was 33 fs, as shown in Fig. 2a. Figure 2b represents a reasonable agreement of the retrieved spectrum from FROG with a directly measured spectrum from a calibrated spectrometer. Figures 2c and 2d are the original and retrieved FROG traces, which converged reasonably well (the error was 0.008).

The well-characterized linearly polarized pulses were passed through a zero-order quarter wave plate in order to vary the polarization state of the beam. The laser beam was focused by a plano-convex lens with a one-meter focal length. The inner diameter of the hollow-core fiber is 400  $\mu\text{m}$ , and it has a length of 90 cm. The fiber was placed on a v-grooved aluminum rod kept in a pressurized chamber filled with Ar gas. The throughput of the fiber was 65–70% for both circular and linear polarization of the input. When the gas was pumped out, the output energy increased linearly as the input energy increased for both the circular and linear inputs, as shown in Fig. 3a. The spatial profiles of the output beam were identical for the circular and the linear input, as shown in Figs. 4a and 4e.

When the gas pressure was 1 bar, the output energy was the same for the two polarization states at very low input energy (0.5 mJ). The output energy did not increase linearly with the input energy for both polarization states, as shown in Fig. 3b. However, the deviation started at a lower input energy for the linear polarization than for the circular polarization. The decrease of throughput with the increase in the input energy was accompanied by the degradation of the spatial profile,

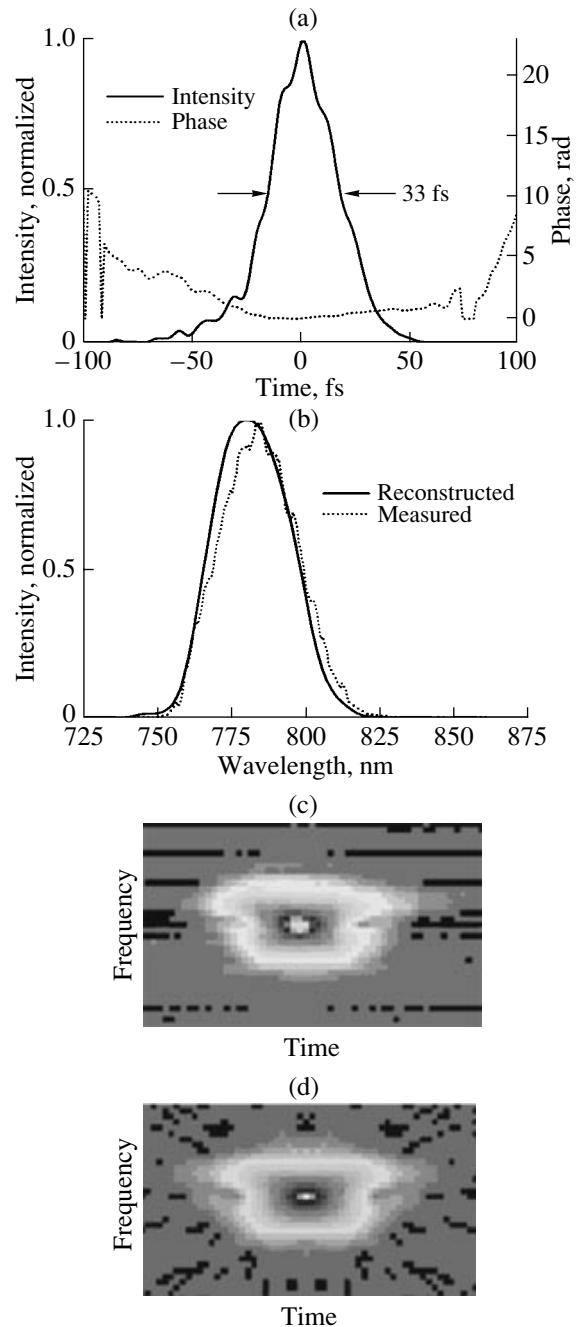


**Fig. 2.** Characterization of the input pulse to the hollow-core fiber with a SHG-FROG. (a) The solid and dotted curves represent the intensity and the phase of the pulse, respectively. (b) The solid curve represents the retrieved spectrum, and the dotted curve represents the measured spectrum. (c) The measured SHG-FROG trace. (d) The reconstructed FROG trace.

as shown in Fig. 4. The spatial profile of the output beam started to degrade at a much lower input energy for the linear polarization than for the circular polarization. For attosecond pulse generation, it is beneficial to use the lowest order spatial mode. For the case under discussion, we define the mode profile in Fig. 4d for the

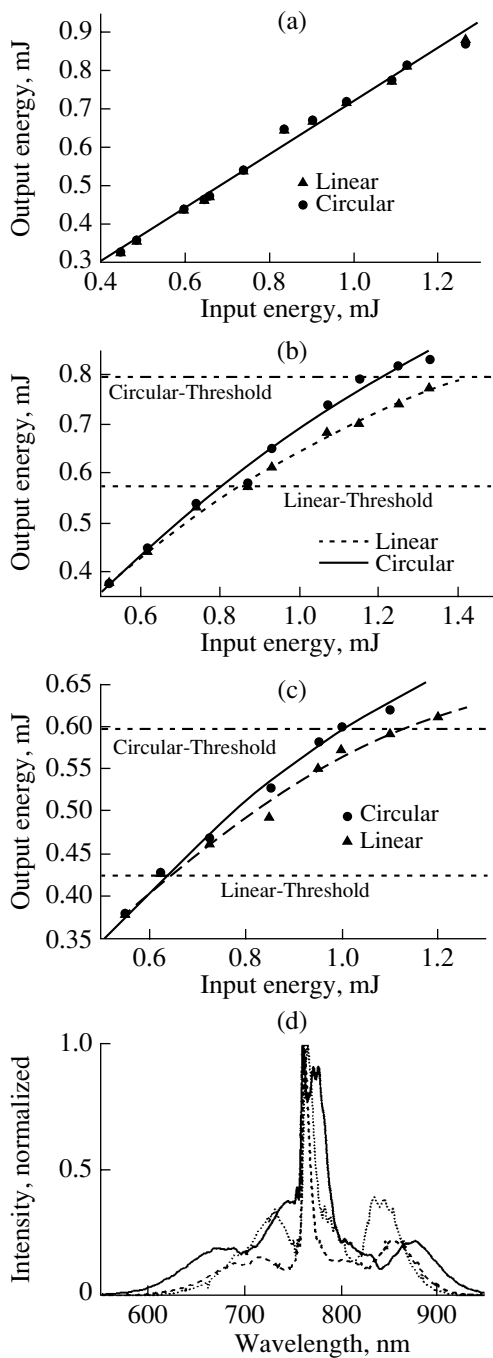


**Fig. 3.** (a)–(c) The circles and triangles represent the measured output energy for the circular and linear polarization input, respectively. The lines are polynomial fitting to the measured data. The Ar gas was zero in (a), 0.5 bar in (b), and 1 bar in (c). (d) The solid line and the dashed lines represent the measured spectra of circularly polarized and linearly polarized output pulses at their thresholds, respectively. The dotted line represents the spectrum with the circular polarization but at the same input energy as of the threshold of the linear polarization.

circular polarization and Fig. 4f for the linear polarization input as the “threshold mode”; i.e., mode profiles better than this are considered acceptable. Using such a

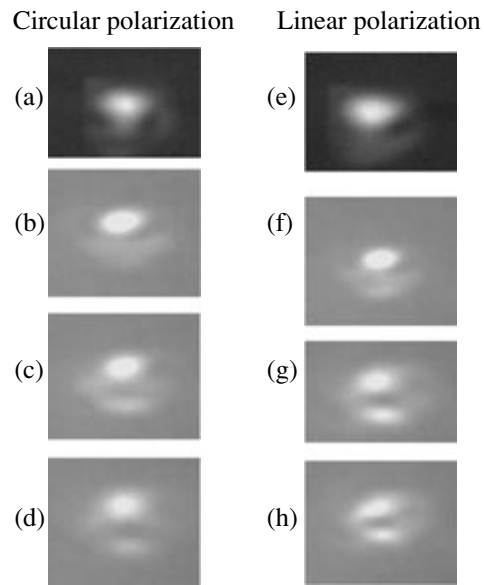


**Fig. 4.** The first and second columns represent the measured spatial profiles of the output beam for the circularly polarized and linearly polarized inputs, respectively. (a) and (e) are the spatial profiles when the gas was pumped out and the input energy was 1.2 mJ. The pairs of (b) and (f), (c) and (g), and (d) and (h) are the measured spatial profiles obtained with input energies of 0.55 mJ, 1 mJ, and 1.2 mJ, respectively. The profile degrades at low input energy for the linear polarization.

definition, the threshold output energy for the circular input was 0.59 mJ, which was 1.3 times higher than for the linear input.

When the gas pressure was 0.5 bar, the dependence of the throughput and spatial profile of the output beam on the input laser energy was similar to that when the pressure was 1 bar. However, the threshold output energy for the circular input was 0.79 mJ, which was 1.5 times higher than for the linear input. Moreover, the spectra of the output pulses were comparable for the two polarization states when the output energies were close to the threshold for the linear input, as shown in Fig. 3d. In the same figure, we present the measured spectrum of the circularly polarized pulses at the threshold energy, which is much broader than that of the linear pulses at threshold. The increase of the threshold by the use of circularly polarized input can be attributed to the suppression of ionization. The spectrum broadening in the fiber is caused mainly by self-phase modulation. Since self-phase modulation and self-focusing are from the same nonlinear effect (the optical Kerr effect), one cannot reduce the self-focusing but maintain the self-phase modulation unchanged to obtain the required bandwidth. The order of nonlinearity of multiphoton ionization is higher than the third-order optical Kerr effect; thus, it can be reduced more effectively when the field is changed from linear to circular polarization.

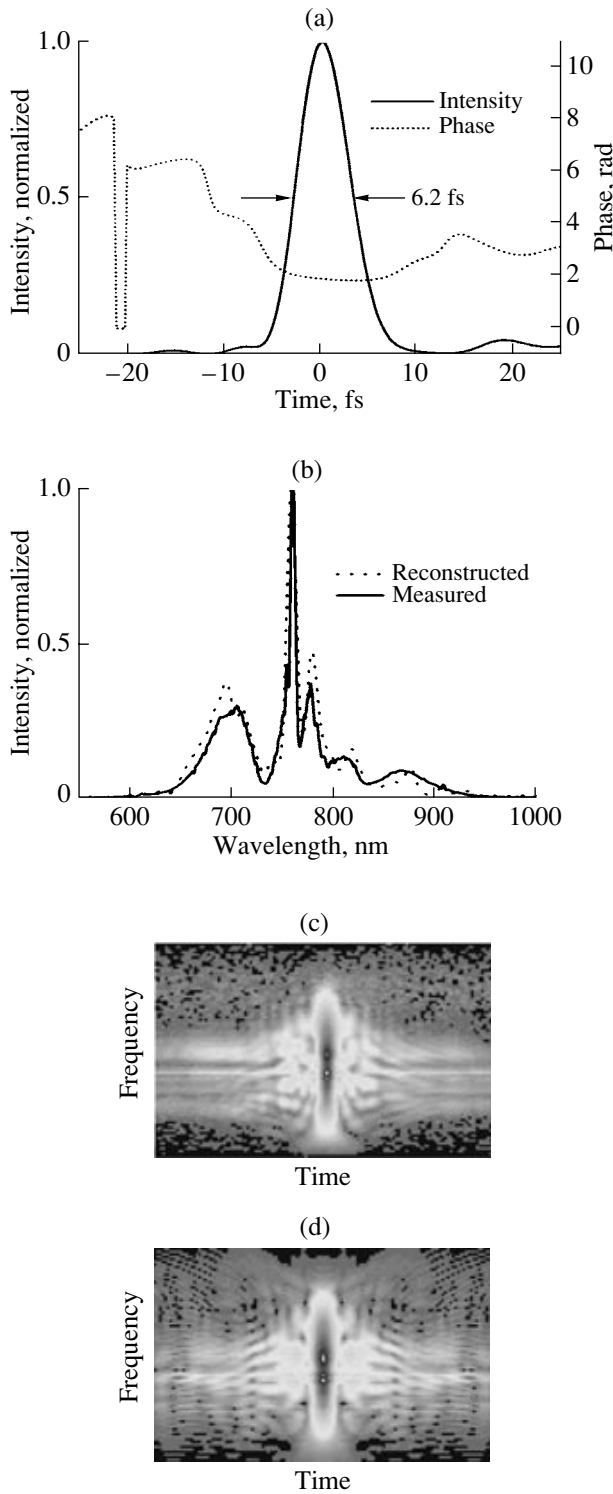


**Fig. 5.** Characterization of the output pulse from the hollow-core fiber with a circular polarization. (a) The solid and dotted curves represent the intensity and the phase of the pulse, respectively. (b) The solid curve represents the retrieved spectrum, and the dotted curve represents the measured spectrum. (c) The measured SHG-FROG trace. (d) The reconstructed FROG trace.

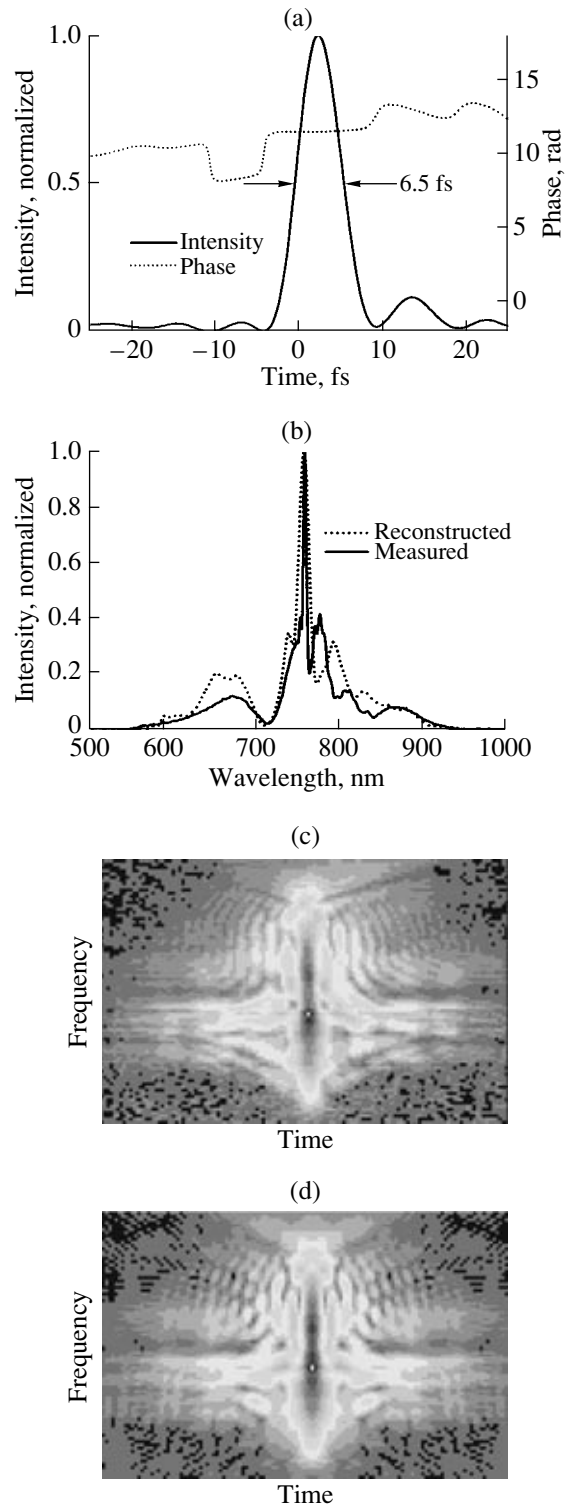


**Fig. 6.** Characterization of the output pulse obtained from the hollow-core fiber with linear polarization. (a) The solid and dotted curves represent the intensity and the phase of the pulse, respectively. (b) The solid curve represents the retrieved spectrum, and the dotted curve represents the measured spectrum. (c) The measured SHG-FROG trace. (d) The reconstructed FROG trace.

The spectrally broadened pulses emerging from the fiber were compressed by using the chirped mirrors. The beam was reflected back and forth on two chirped mirrors. The total number of reflections was six, which introduced a GVD of  $\sim 300$  fs<sup>2</sup>. The amount of negative GVD introduced by the chirped mirrors was sufficient to compensate for the self-phase modulation inside the fiber and the material dispersion from the output end of the fiber to the FROG. The dispersion includes the exit window of the fiber chamber (0.5 mm of fused silica), five meters of air, a beam splitter in the SHG-FROG, and 0.5 mm of fused silica plate placed at the input of the FROG. The thickness of the plate was chosen to yield the shortest pulse. The direction of the beam was kept perpendicular to the chirped mirrors to ensure similar compensation on both the *s* and *p* components of the circularly polarized pulse. After the chirped mirror, the beam was collimated with a concave mirror with a radius of curvature of five meters. The diameter of the collimated beam was 1 cm. When the input beam was circularly polarized, the pulse energy after the chirped mirrors and the collimation mirrors was 0.6 mJ at the threshold. The field strength of the input circularly polarized pulses was equal in all directions, with an error of  $\pm 5\%$ . We characterized the vertical component of the compressed pulses using SHG-FROG.

The characterization of compressed pulses was done using the SHG-FROG as described earlier. It was a challenge to measure the sub-ten-femtosecond pulses with a FROG because of the broader spectrum. The spectral responses of the spectrometer and the CCD camera were calibrated with a Deuterium lamp. This allowed for the correction of the measured signal. A 5- $\mu$ m-thick BBO was used in the FROG so that the phase-matching bandwidth could accommodate the spectrum of the pulse. When the input pulse was circularly polarized and its energy is at the threshold, the measured pulse was 6.2 fs at FWHM, as shown in Fig. 5a. The retrieved spectrum from FROG agreed reasonably well with the measured spectrum from a calibrated spectrometer, as shown in Fig. 5b. This ensures the reliability of the measurement. Figures 5c and 5d are the measured and retrieved traces. As a comparison, the compressed pulse shape corresponding to the linearly polarized input is presented in Fig. 6. Although the spectrum of the circular pulse could support even shortened pulses, the quality of the chirped mirrors used here cannot compensate the GVD over the whole spectral range, which can be seen from the FROG trace.

In conclusion, we have demonstrated a simple way to scale up the output energy from the hollow-core fiber/chirped mirror compressor technique. When the

fiber chamber was filled with 0.5-bar argon gas, the output energy with circular polarization was 1.5 times higher than with a linear polarization for a similar spatial mode and pulse duration. The improvement can be attributed to the reduction of the ionization by using circularly polarized pulses. The maximum energy of the compressed circularly polarized pulses was 0.6 mJ, which was the highest energy achieved in argon with pulse durations of less than 7 fs. We expect that this idea is effective for other gases, such as neon, so that an even higher energy could be obtained. This discovery will have a great impact on attosecond pulse generation by polarization gating and for reaching a higher cutoff photon energy in high-harmonic generation.

#### ACKNOWLEDGMENTS

This work was supported by the Division of Chemical Sciences, Office of Basic Energy Sciences, US Department of Energy.

#### REFERENCES

1. T. Brabec and F. Krausz, *Rev. Mod. Phys.* **72**, 545 (2000).
2. P. M. Paul, E. S. Toma, P. Breger, *et al.*, *Science* **292**, 1689 (2001).
3. Hiromichi Niikura, F. Legaré, R. Hasbani, *et al.*, *Nature* **421**, 286 (2003).
4. B. Shan, S. Ghimire, and Z. Chang, *J. Mod. Opt.* **52**, 277 (2005).
5. A. Baltuska, Th. Udem, M. Uiberacker, *et al.*, *Nature* **421**, 611 (2003).
6. M. Yu. Emelin, M. Yu. Ryabikin, A. M. Sergeev, *et al.*, *JETP Lett.* **77**, 212 (2003).
7. Zenghu Chang, *Phys. Rev. A* **70**, 043 802 (2004).
8. B. Shan, S. Ghimire, and Z. Chang, *OSA* (2003).
9. M. Nisoli, S. Stagira, S. De Silverstri, *et al.*, *Appl. Phys. B* **65**, 189–196 (1997).
10. S. Sartania, Z. Cheng, M. Lenzner, *et al.*, *Opt. Lett.* **22**, 20 (1997).
11. M. Nurthuda, A. Suda, M. Hatayama, *et al.*, *Riken Rev.* **49**, 10 (2002).
12. G. Fibich and A. L. Gaeta, *Opt. Lett.* **25**, 5 (2000).
13. B. Shan, S. Ghimire, and Zenghu Chang, *Phys. Rev. A* **69**, 021404 (2004).
14. Patrick O'Shea, Mark Kimmel, Xun Gu, and Rick Trebino, *Opt. Express* **7** (10), 1276 (2000).
15. S. Stagira, E. Priori, G. Sansone, *et al.*, *Phys. Rev. A* **66**, 033810 (2002).